Clinical Neurology and Neurosurgery 185 (2019) 105491

Contents lists available at ScienceDirect

Clinical Neurology and Neurosurgery

journal homepage: www.elsevier.com/locate/clineuro

Radiomics features on non-contrast computed tomography predict early enlargement of spontaneous intracerebral hemorrhage

Hui Li[a], Yuanliang Xie[a,*], Xiang Wang[a], Faxiang Chen[a], Jianqing Sun[b], Xiaoli Jiang[a]

[a] Department of Radiology, Central Hospital of Wuhan, Tongji Medical College, Huazhong University of Science and Technology, Wuhan, Hubei Province 430014, China
[b] Philips Healthcare, Shanghai 510530, China

ARTICLE INFO

Keywords:
Radiomics
Intracerebral hemorrhage
Enlargement
Computed tomography
Algorithms

ABSTRACT

Objective: To explore the value of radiomics features on non-contrast computed tomography (NCCT) in predicting early enlargement of spontaneous intracerebral hemorrhage (SICH).

Patients and Methods: 167 patients with SICH were divided into enlarged hematoma and non-enlarged hematoma groups based on the volume of hematoma on 24-h follow-up CT images > 30% and/or 6 ml of the baseline NCCT. The baseline NCCT images of all cases were imported into radiomics software to extract the radiomics features of the initial hematoma. For each case, the features with good predictability were retained after the feature-selected process; the remaining features were used to construct model with 23 algorithms one-by-one. A 5-fold method was used to cross-validate the model and repeated 5 times. The algorithm model with the highest accuracy was selected as predictive model for hematoma enlargement (HE) in SICH, its average parameters including AUC, accuracy, sensitivity, specificity, F1 score, positive predictive value (PPV), negative predictive value (NPV), false positive rate (FPR), false negative rate (FNR),and false discovery rate (FDR) were taken as evaluating indicators.

Results: A total of 1227 texture features of each cerebral hematoma were obtained. After the feature-selected process, 4 features (wavelet-LHL mean, wavelet-LLL _ Idm, wavelet-LLL _run length non-uniformity normalized, and wavelet-LLL _contrast) remained to construct the predictive models. Among 23 model algorithms, Linear Support Vector Classifier showed the highest accuracy (72.6%), and eventually was selected as the predictive model, its AUC, accuracy, sensitivity, specificity, F1 score, PPV, NPV, FPR, FNR, and FDR were 0.729, 0.726,0.717,0.736,0.714, 0.736, 0.741, 0.264, 0.283 and 0.264, respectively.

Conclusion: Radiomics features of cerebral hematoma on baseline NCCT images showed good performance in predicting HE of SICH.

1. Introduction

Spontaneous intracerebral hemorrhage (SICH) is a blood clot that arises in the brain parenchyma in the absence of trauma or surgery, it accounts for 10%–15% of all strokes [1,2] and is associated with higher mortality rate (44%–50%) [3]. Nearly one-third of SICH patients will develop hematoma enlargement (HE) most commonly in the first several hours after symptom onset [4–7], which related to worse clinical outcomes [8]. Therefore, effective prediction for HE is of great significance for timely intervention and improvement of patient prognosis.

Non-contrast computed tomography (NCCT) scanning is the first diagnostic procedure of choice in patients with acute stroke [1]. Previous studies have identified various heterogeneity signs based on NCCT images as predictors for HE, including the swirl sign, blend sign, and black hole sign [9], which consistently emphasize hypo- or iso-attenuation regions within hyper-attenuated hematomas. Indeed, the heterogeneous signs of hypo- or iso-attenuation regions may indicate fresh bleeding [10]. Although the NCCT signs mentioned above are accepted predictors worldwide, the assessment of the signs is inevitably subjective. In addition, despite the proposed grading system based on NCCT for prediction of HE [11], the evaluation is still semi-quantitative and the sensitivity and accuracy are restricted. Therefore, we need to find more quantitative, sensitive, and accurate heterogeneous markers on NCCT images as new predictors for HE.

Radiomics, the high-throughput extraction of large amounts of image features from radiographic images, is a new, quantitative approach for image analysis [12]. In the last few years, radiomics has been mainly used in the field of tumor heterogeneous research and has given

* Corresponding author: Department of Radiology, Central Hospital of Wuhan, Tongji Medical College, Huazhong University of Science and Technology, No. 26 Shengli Street, Jiangan District, Wuhan City, Hubei Province 430014, China.
E-mail address: huilee1987_1_9@126.com (Y. Xie).

https://doi.org/10.1016/j.clineuro.2019.105491
Received 27 May 2019; Received in revised form 24 July 2019; Accepted 14 August 2019
Available online 15 August 2019

rise to contributions in tumor diagnosis, classification, prediction of tumor outcomes, and therapeutic effects. For example, Liang et al. [13] adopted a supervised learning method to analyze the CT images of 494 patients with colorectal cancer and showed that a radiomics signature was validated as a significant predictor for discrimination between stages I-II and III-IV colorectal cancer.

Few studies, however, have predicted HE in SICH using a radiomics approach to date. We introduce radiomics imaging analytic method based on NCCT in this study to quantify the heterogeneity of hematomas in order to find more quantitative, sensitive, and accurate indicators for predicting HE.

2. Materials and methods

2.1. Patients

This study was approved by the local Medical Ethics Committee of Wuhan Central Hospital. We retrospectively collected 215 cases of patients with SICH from May 2017 to February 2019. All patients underwent baseline NCCT within 6 h after the onset of symptoms and had a follow-up CT evaluation at 24 h. The exclusion criteria were as follows: (1) cerebral hemorrhage caused by trauma, aneurysms, vascular malformations, venous sinus emboli, and tumors; (2) isolated ventricular, subdural, or epidural hemorrhage;(3) hematoma removal surgery before the 24-h follow-up CT; and (4) CT images with artifacts. Of the 215 intracranial hematoma cases, 48 cases were excluded, and 167 cases were included in this study.

Clinical data were collected, including age, gender, admission systolic blood pressure, Glasgow score, time to baseline NCCT and initial volume of the hematoma.

2.2. CT imaging acquisition

A second generation 128-slice dual-source CT scanner (Siemens, Somatom Definition, Germany) was used for the NCCT scan. The scanning range was from the skull base to the top with scan thickness of 5 mm, a tube current of 587 mAs, a tube voltage of 120 KV, a field of view (FOV) of 25 cm, and a matrix size of 512 × 512.

2.3. Hematoma volume calculation and grouping

Hematoma volumes on the baseline NCCT and 24-h follow-up CT were calculated according to the following formula: $A \times B \times C/2$ [14]. HE was defined as the volume of hematoma on 24-h follow-up CT images > 30% and/or 6 ml on the baseline NCCT [15]. After volumes calculated, 42 cases were divided to the HE group and 125 cases were non-HE group.

2.4. Hematoma delineation and segmentation

The baseline NCCT images were derived from the Picture Archiving and Communication System (PACS) with a uniform window position of 35 HU and a window width of 90 HU. The baseline NCCT images were imported to In-home radiomics tool base on Mat-Lab software (Philips_Radiomics_v93; Philips Investment Co., Ltd., Shanghai, China) to obtain texture features. The outlines of all cerebral hematomas were drawn manually layer-by-layer and the three-dimensional volumes of interest (VOIs) were formed, then a large number of texture parameters of the VOIs were automatically calculated. The process of hematoma delineation and segmentation is showed in Fig. 1.

Image analysis was performed by an experienced radiologist and a resident. Twenty patients were randomly selected to evaluate the consistency of the surveyor and between the surveyors. The twenty hematomas were first drawn by physician 1, then re-drawn by the same physician 1 week later. Physician 2 drew the outlines of the 20 hematomas only once.

2.5. Radiomics features extraction

A total of 1227 radiomics features were obtained for each case. Texture features were divided into four groups. Group 1 included 17 shape-based features reflecting the shape and size of the target region. Group 2 covered 19 first order texture features reflecting gray-scale histogram information.5 types based on the calculations obtained from the grey level co-occurrence matrix(GLCM), gray level size zone matrix (GLSZM), and grey level run length matrix(GLRLM), neighborhood grey-tone difference matrix(NGTDM), and grey level dependent matrix (GLDM) were classified to Group 3, 75 features in all. Group 4 (higher-order features), with 1116 features, included the intensity and texture features in Group 3 that were derived from the wavelet transformation and the filters of exponential, square, squareroot, logarithm, laplacian.

2.6. Radiomics features selection and machine learning

The radiomics features analysis was implemented by Python software. A machine learning algorithm was used to analyze texture features and another sampling algorithm was applied to balance the data of different classes and randomly selected 42 of 125 non-HE patients. Eighty-four patients (42 HE and 42 non-HE patients) were included in the following analysis.

Radiomics features selection:

All features for each case were first analyzed by Pearson correlation with the classification labels, and the features with label correlation coefficient > 0.2 and $p < 0.1$ were retained. The retained features were used for clustering analysis and those with correlation > 0.75 were defined as highly similar features, the redundant features with high similarity were removed and the final remaining features were used to establish predictive models.

Model construction and selection:

The remaining features were used to construct model with 23 algorithms one-by-one.

The retained features were used to construct models with 23 model algorithms one-by-one. 5-fold method (all cases were divided into 5 parts, 4 parts used for model training,1 part used for validation) was used to cross-validate the models and repeated 5 times. The average predictive parameters were obtained after training, and the model with the highest accuracy was selected as predictive model. The parameters of predictive model including AUC, accuracy, sensitivity, specificity, F1 score, PPV, NPV, FPR, FNR, and FDR were used to evaluate the diagnostic efficacy in predicting HE.

The flow chart of radiomics features extraction and analysis is showed in Fig. 2.

3. Statistical analysis

IBM SPSS Statistics 22 statistical analysis software (New York, USA) was used to perform the statistical analysis. The categorical/dichotomous variables (gender) were analyzed using a χ^2 test, and continuous variables (age, admission systolic blood pressure, Glasgow score, time to baseline NCCT, and volume of the initial hematoma) were analyzed by *t*-test or Mann-Whitney U test; $p < 0.05$ was considered to represent a statistically significant difference.

Using the intraclass correlation coefficient(ICC)to evaluate the consistency of the surveyor and between the surveyors. ICC < 0.4

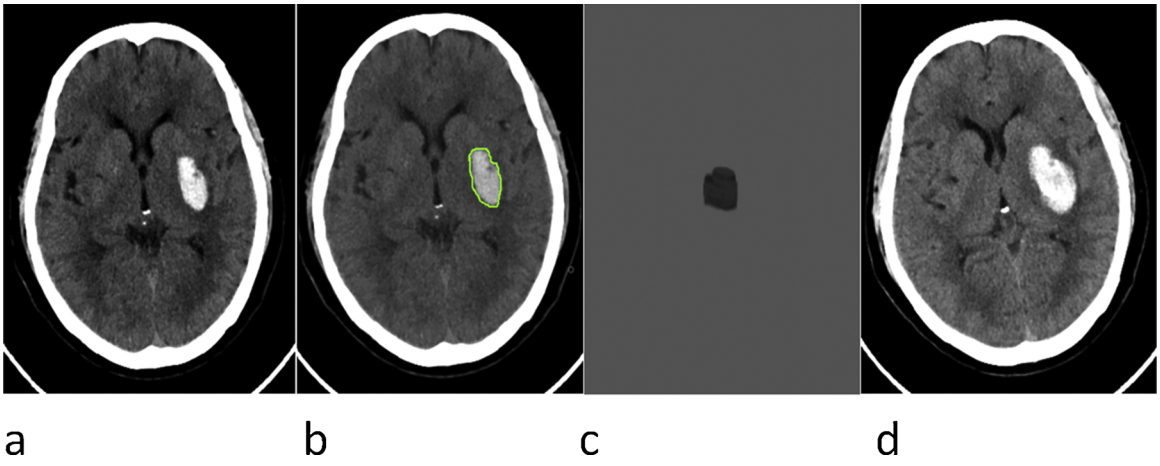

Fig. 1. a: The basal ganglia hematoma on baseline NCCT images. b: Hematoma delineation and segmentation. c: The three-dimensional volume of hematoma after segmentation. d: The hematoma developed enlargement on 24-h follow-up NCCT.

indicated the reliability of the data was poor, while ICC > 0.75 suggested high data credibility.

4. Results

4.1. Clinical characteristics

Despite the time to baseline CT significant difference between the two groups (2.0[1.0–2.0] vs 2.0[1.5–4.0]; p = *0.009*),there were no significant differences in gender (male%) (69.05% vs 59.20%), age (57.31±11.41 vs 59.11±12.84), admission systolic blood pressure (171.21±25.48 vs 168.41±26.40),Glasgow score(11[7–13.5] vs 14[12.5–15]), and initial volume of the hematoma(20.20±20.46 vs 14.86±14.08) between the groups (p > 0.05)*(*Table 1*)*.

4.2. Radiomics features selection

After Pearson correlation analysis and clustering analysis, four texture features (FirstOrder_wavelet_LHL_Mean,GLCM_wavelet_LLL_Idm,GLCM_wavelet_LLL_Contrast,GLRLM_wavelet-LLL_RunLengthNonUniformityNormalized)were retained for building models(the definition of the features can be found at https://pyradiomics.readthedocs.io).

Table 1
Comparison of clinical data between two groups. *$p < 0.05$.

Clinical variables	HE group	Non-HE group	*P* value
Gender, male (%)	29(42)	74(125)	0.256
Age, years (mean±SD)	57.31±11.41	59.11±12.84	0.420
ASBP(mm Hg)	171.21±25.48	168.41±26.40	0.543
Time to baseline CT(h)	2.0(1.0-2.0)	2.0(1.5-4.0)	0.009*
GCS(score)	11(7-13.5)	14(12.5-15)	0.119
Initial hematoma volume(ml)	20.20±20.46	14.86±14.08	0.061

4.3. Diagnostic performance of the radiomics model

After cross-validation training with 5-fold method repeated five times, Linear Support Vector Classifier showed the highest accuracy of 72.6% among the 23 model algorithms (Fig. 3), so we selected Linear Support Vector Classifier as predictive model. Fig. 4 shows the confusion matrix - cross-validation database of Linear Support Vector Classifier.

The accuracy, sensitivity, specificity, F1 score, PPV, NPV, FPR, FNR, and FDR of Linear Support Vector Classifier in predicting HE are 0.726, 0.717, 0.736, 0.714, 0.736, 0.741, 0.264, 0.283, and 0.264, respectively (Fig. 5). Fig. 6 shows five ROC curves after cross-validation training five times, average ROC curve (blue color) and their respective

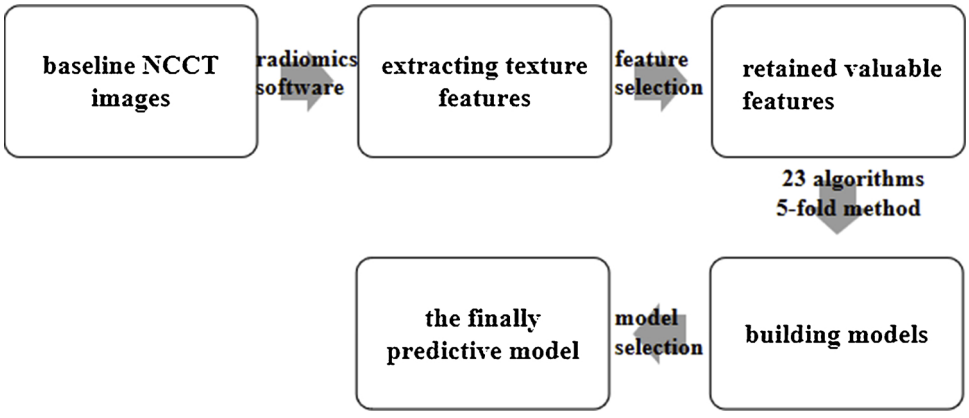

Fig. 2. The flow chart of texture analysis.

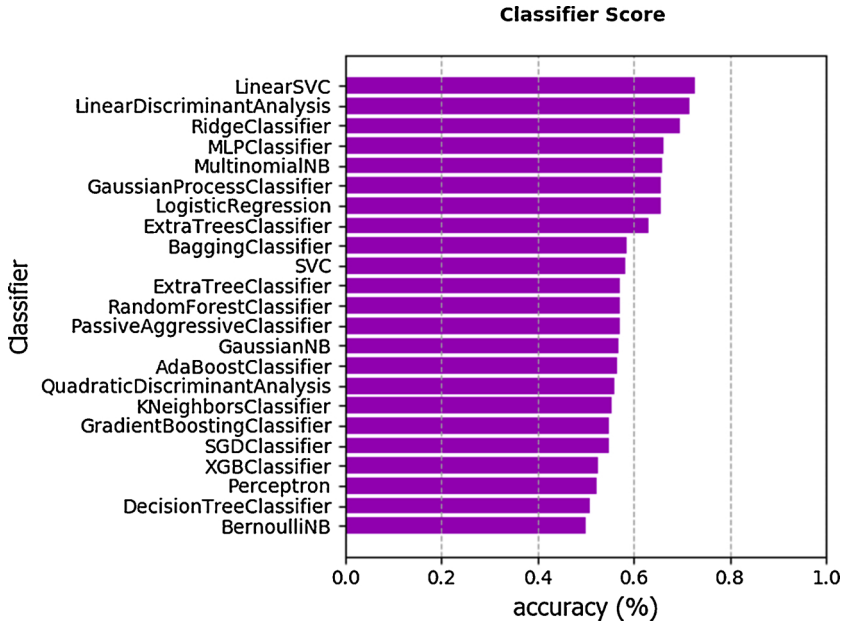

Fig. 3. Accuracy ranking of 23 model algorithms.

AUC values (0.74, 0.88, 0.58, 0.66, 0.79, 0.73 ± 0.10, respectively).

4.4. The consistency of the surveyor and between the surveyors

The radiomics features obtained twice by physician 1 were compared, and the ICCs were between 0.786 and 0.998 which indicated satisfactory consistency for the surveyor himself (Table 2). The features extracted by physician 1 at first time were compared to those measured by physician 2 and the ICCs were between 0.878 and 0.972, also indicated a superior consistency (Table 3).

5. Discussion

This study built predictive models based on radiomics features filtered by Pearson correlation analysis and clustering analysis, the result illustrated that Linear Support Vector Classifier showed a good performance in predicting HE. Like previous studies [16–19], this study further confirmed that the heterogeneity of the hematoma was helpful in predicting HE. Previous studies have proposed several effective NCCT heterogeneity markers, such as the blend, swirl, and black hole signs. These signs describe different hypo- or iso-attenuation regions within the hyper-attenuated hematoma [20]. The heterogeneity on CT attenuation of hematomas depends on the time course of hemorrhage, therefore the hypo- or iso- and hyper-attenuation areas reflect different stages of hemorrhage. The hyper-attenuation areas represent coagulated and contracted clots, while the hypo- or iso-attenuation regions represent fresh bleeding [21,22]. So, the more active bleeding points in the hematoma, the more hypo- or iso-attenuation regions, and the greater the heterogeneity of the hematoma. The occurrence of HE may present a cascade reaction of continuous active bleeding within the initial hematoma that results in the rupture of peripheral blood vessels [23,24], there are often one or more active bleeding points in and around the enlarged hematoma, so the heterogeneity of the hematoma with a tendency to enlarge may be greater than that of a stable hematoma. This study showed that radiomics features can reliably distinguish between hematomas with a tendency to enlarge from stable hematomas, the difference in heterogeneity between the two types might be the main cause.

Among the previously proposed NCCT heterogeneous markers, the black hole sign showed the best predictive value (AUC = 0.641˜0.646, sensitivity = 33.8%˜43.75%) [20,25]. The black hole sign was defined as: hypo-attenuation areas (black holes) with round, oval or rod shape, recognizable boundaries and not connected to adjacent brain tissues encapsulated in hyper-attenuation hematomas. Obviously, it is a subjective indicator. The radiomics method introduced in this study could quantitatively extract heterogeneous parameters of hematoma and avoid subjectivity. Our result showed the AUC and sensitivity of the NCCT texture features in predicting HE were 0.729 and 71.7%, significantly higher than the black hole sign. The reasons may be as follows: firstly, NCCT texture features are quantitative indicators and more objectively, more accurately than black hole sign; secondly, the black hole sign is a single and macroscopic indicator, while NCCT texture features are a large number of micro-indicators, which give a more comprehensive and accurate evaluation.

Previous studies reported that the spot sign is more accurate and sensitive than NCCT markers in predicting HE [26,27], recommended as an independent predictor of HE [28–30]. The spot sign refers to one or more foci of contrast enhancement within an acute primary parenchymal hematoma that is visible on CT images after injection of contrast medium [31], reflecting continuous bleeding of ruptured vessels. The pathophysiology underlying the spot sign is still unclear, but could involve progressive small vessel damage following SICH [32]. The sensitivity of the spot sign for predicting HE varied greatly, ranging from 57.14%–91%, so how the sensitivity it is controversial. In addition, the incidence of spot signs is low (20%–30% of patients with SICH undergoing CTA scans) [28,33]. Moreover, the appearance of the spot sign relies on CTA, CTP, or an enhanced CT examination, which depend injection of a contrast agent, more expensive, time-consuming, and a larger radiation dose than NCCT, therefore it's not recommended as the first choice in clinic [9]. Sporns et al. [27] compared the predictive value of NCCT heterogeneity signs with CTA point signs for HE and found that NCCT heterogeneity signs showed a good correlation with spot sign, which indicated that spot sign may have the same pathophysiologic basis as the hypo- or iso-attenuation regions on NCCT.

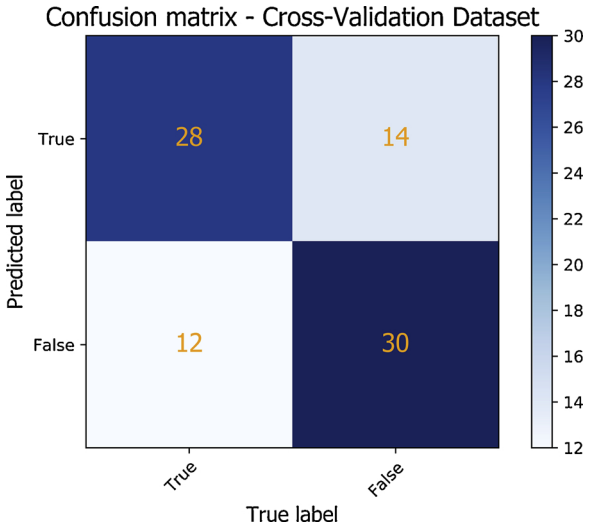

Fig. 4. The confusion matrix -cross-validation database of Linear Support Vector Classifier.

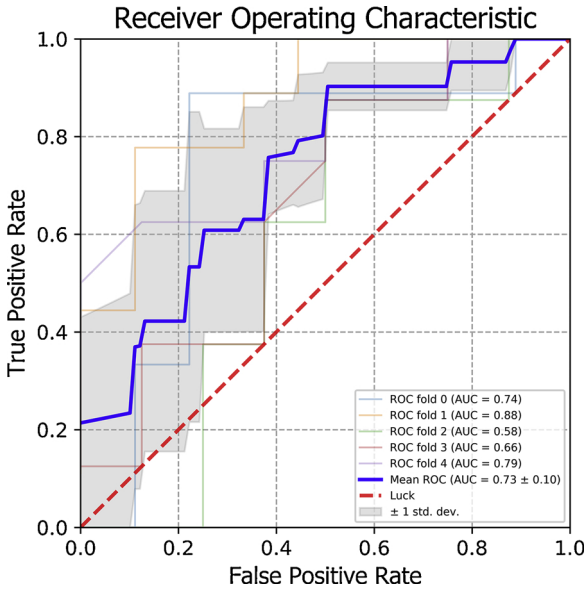

Fig. 6. The ROC curve of Linear Support Vector Classifier in predicting HE.

Therefore, in general, it is more significant to study the heterogeneity of hematoma on baseline NCCT than contrast CT. In fact, our study further confirmed that heterogeneity of hematoma on NCCT indeed has high value in predicting HE.

There are some limitations in this study. First, this study was retrospective design from a single-center and the sample size was small, a larger prospective multi-center study is needed to provide more insight in this issue. Second, we used ABC/2 scores with 5mm-thickness-slice to determine the volume of intracranial hematoma, and this formulator is sufficiently accurate when the hematoma at local or central sites,

a

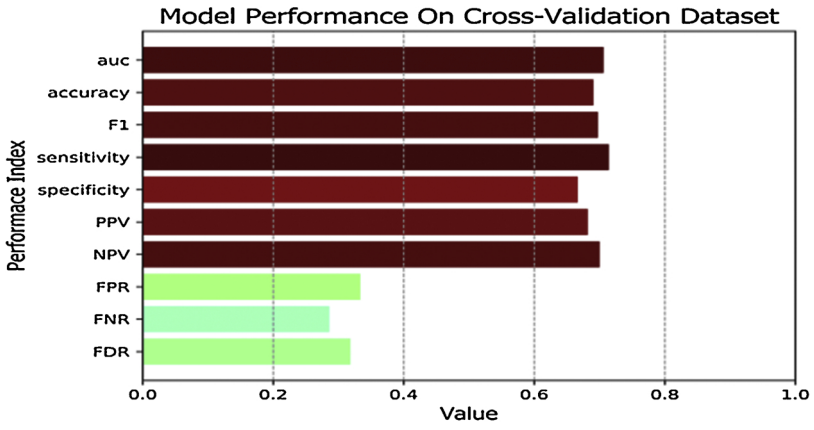

b

Performances from 5-fold Cross-validation

Criterion	Value
Mean AUC	0.729
Mean Accuracy	0.726
Mean Sensitivity	0.717
Mean Specificity	0.736
F1	0.714
PPV	0.736
NPV	0.741
FPR	0.264
FNR	0.283
FDR	0.264

Fig. 5. a,b: The average predictive parameters of Linear Support Vector Classifier.

Table 2
The consistency analysis of texture parameters measured twice by physician 1.

Texture features	ICC	95%CI
FirstOrder_wavelet_LHL_Mean	0.786	0.307-0.947
GLCM_wavelet_LLL_Idm	0.907	0.644-0.978
GLCM_wavelet_LLL_Contrast	0.904	0.635-0.978
GLRLM_wavelet-LLL_RunLengthNonUniformityNormalized	0.998	0.990-0.999

Table 3
The consistency analysis of texture parameters measured by two physicians.

Texture features	ICC	95%CI
FirstOrder_wavelet_LHL_Mean	0.900	0.649-0.974
GLCM_wavelet-LLL_Idm	0.965	0.867-0.991
GLCM_wavelet_LLL_Contrast	0.878	0.585-0.968
GLRLM_wavelet-LLL_RunLengthNonUniformityNormalized	0.972	0.892-0.993

however, accuracy decreases with large, irregular, or lobar clots, thus volumetric 3-D analysis with thinner-slice images might be a best choice if time-consuming is not in consideration, and we expect computer-aid sketching method should be explored in the future. Third, manual defined ROIs need a few additional minutes for radiomics analysis, but prediction of hematoma with enlargement risk could be benefit for treatment strategy. Moreover, this study is a preliminary study on the feasibility of using radiomics method to predict HE, so no specific texture features have been established as predictors. Our study has proved that radiomic method is helpful in predicting HE, so we will further look for specific radiomic features and the cut off values for predicting HE in future studies.

6. Conclusion

In conclusion, Linear Support Vector Classifier based on four radiomic features (FirstOrder_wavelet_LHL_Mean,GLCM_wavelet_LLL_Idm,GLCM_wavelet_LLL_Contrast,GLRLM_wavelet-LLL_RunLengthNonUniformityNormalized) from NCCT images showed a good performance in predicting HE, it's more objective, fast, acceptable and comprehensive than previous NCCT heterogeneity markers and the spot sign. The method of radiomics texture analysis from NCCT images might provide guidance for clinical individualized treatment.

Ethics approval and consent to participate

The study was approved by the local Medical Ethics Committee of Wuhan Central Hospital. Informed consent was obtained.

Consent for publication

Not applicable.

Availability of data and material

Not applicable.

Funding

None.

Declaration of Competing Interest

There are no potential conflicts of interest to disclose.

Acknowledgements

Not applicable.

References

[1] M.E. Fewel, B.G. Thompson Jr, J.T. Hoff, Spontaneous intracerebral hemorrhage: a review, Neurosurg. Focus 15 (4) (2003) E1, https://doi.org/10.3171/foc.2003.15.4.1.
[2] A.I. Qureshi, S. Tuhrim, J.P. Broderick, H.H. Batjer, H. Hondo, D.F. Hanley, Spontaneous intracerebral hemorrhage, N. Engl. J. Med. 344 (19) (2001) 1450–1460.
[3] J.P. Broderick, T. Brott, T. Tomsick, R. Miller, G. Huster, Intracerebral hemorrhage more than twice as common as subarachnoid hemorrhage, J. Neurosurg. 78 (2) (1993) 188–191, https://doi.org/10.3171/jns.1993.78.2.0188.
[4] T. Brott, J. Broderick, R. Kothari, W. Barsan, T. Tomsick, L. Sauerbeck, J. Spilker, J. Duldner, J. Khoury, Early hemorrhage growth in patients with intracerebral hemorrhage, Stroke 28 (1) (1997) 1–5, https://doi.org/10.1161/01.STR.28.1.1.
[5] Y. Fujii, R. Tanaka, S. Takeuchi, T. Koike, T. Minakawa, O. Sasaki, Hematoma enlargement in spontaneous intracerebral hemorrhage, J. Neurosurg. 80 (1) (1994) 51–57, https://doi.org/10.3171/jns.1994.80.1.0051.
[6] S. Kazui, K. Minematsu, H. Yamamoto, T. Sawada, T. Yamaguchi, Predisposing factors to enlargement of spontaneous intracerebral hematoma, Stroke 28 (12) (1997) 2370–2375, https://doi.org/10.1161/01.STR.28.12.2370.
[7] S. Kazui, H. Naritomi, H. Yamamoto, T. Sawada, T. Yamaguchi, Enlargement of spontaneous intracerebral hemorrhage: incidence and time course, Stroke 27 (10) (1996) 1783–1787, https://doi.org/10.1161/01.STR.27.10.1783.
[8] E.C. Jauch, C.J. Lindsell, O. Adeoye, J. Khoury, W. Barsan, J. Broderick, A. Pancioli, T. Brott, Lack of evidence for an association between hemodynamic variables and hematoma growth in spontaneous intracerebral hemorrhage, Stroke 37 (8) (2006) 2061–2065, https://doi.org/10.1161/01.STR.0000229878.93759.a2.
[9] D.F. Zhang, J.G. Chen, Q. Xue, Li Y. Du BY, T. Chen, Y. Jiang, L.J. Hou, Y. Dong, J.Y. Wang, Heterogeneity Signs on Noncontrast Computed Tomography Predict Hematoma Expansion after Intracerebral Hemorrhage: A Meta-Analysis, Biomed Res. Int. 2018 (2018) 6038193, https://doi.org/10.1155/2018/6038193 eCollection2018.
[10] X. Xiong, Q. Li, W.S. Yang, X. Wei, X.C. Wang, D. Zhu, R. Li, D. Cao, P. Xie, Comparison of swirl sign and black hole sign in predicting early hematoma growth in patients with spontaneous intracerebral hemorrhage, Med. Sci. Monit. 24 (2018) 567–573, https://doi.org/10.12659/MSM.906708.
[11] Y.W. Huang, Q. Zhang, M.F. Yang, A reliable grading system for prediction of hematoma expansion in intracerebral hemorrhage in the basal ganglia, Biosci. Trends 12 (2) (2018) 193–200, https://doi.org/10.5582/bst.2018.01061.
[12] P. Lambin, E. Rios-Velazquez, R. Leijenaar, S. Carvalho, R.G. van Stiphout, P. Granton, G.M. Zegers, R. Gillies, R. Boellard, A. Dekker, H.J. Aerts, Radiomics: Extracting more information from medical images using advanced feature analysis, Eur. J. Cancer 48 (4) (2012) 441–446, https://doi.org/10.1016/j.ejca.2011.11.036.
[13] C.S. Liang, Y.Q. Huang, L. He, X. Chen, Z.L. Ma, D. Dong, J. Tian, C.H. Liang, Z.Y. Liu, The development and validation of a CT-based radiomics signature for the preoperative discrimination of stage I-II and stage III-IV colorectal cancer, Oncotarget 7 (21) (2016) 31401–31412, https://doi.org/10.18632/oncotarget.8919.
[14] R.U. Kothari, T. Brott, J.P. Broderick, W.G. Barsan, L.R. Sauerbeck, M. Zuccarello, J. Khoury, The ABCs of measuring intracerebral hemorrhage volumes, Stroke 27 (8) (1996) 1304–1305, https://doi.org/10.1161/01.STR.27.8.1304.
[15] A. Ederies, A. Demchuk, T. Chia, D. Gladstone, D. Downlatshahi, G. Bendavit, K. Wong, S.P. Symons, R.I. Aviv, Postcontrast CT extravasation is associated with hematoma expansion in CTA spot negative patients, Stroke 40 (2009) 1672–1676, https://doi.org/10.1161/STRO-KEAHA.108.541201.

[16] E. Selariu, E. Zia, M. Brizzi, K. Abul-Kasim, Swirl sign in intracerebral haemorrhage: definition,prevalence, reliability and prognostic value, BMC Neurol. 12 (109) (2012) 1–6, https://doi.org/10.1186/1471-2377-12-109.
[17] W.J. Wang, N.Q. Zhou, C. Wang, Early-stage estimated value of blend sign on the prognosis of patients with intracerebral hemorrhage, Biomed Res. Int. 2018 (2018), https://doi.org/10.1155/2018/4509873.eCollection 2018 4509873.
[18] Q. Li, W.S. Yang, X.C. Wang, D. Cao, D. Zhu, F.J. Lv, Y. Liu, L. Yuan, G. Zhang, X. Xiong, R. Li, Y.X. Hu, X.Y. Qin, P. Xie, Blend sign predicts poor outcome in patients with intracerebral hemorrhage, PLoS One 12 (8) (2017), https://doi.org/10.1371/journal.pone.0183082 e0183082.
[19] Q. Li, G. Zhang, X. Xiong, X.C. Wang, W.S. Yang, K.W. Li, X. Wei, P. Xie, Black hole sign:novel imaging marker that predicts hematoma growth in patients with intracerebral hemorrhage, Stroke 47 (7) (2016) 1777–1781, https://doi.org/10.1161/STROKEAHA.116.013186.
[20] X. Xiong, Q. Li, W.S. Yang, X. Wei, X. Hu, X.C. Wang, D. Zhu, R. Li, D. Cao, P. Xie, Comparison of swirl sign and black hole sign in predicting early hematoma growth in patients with spontaneous intracerebral hemorrhage, Med. Sci. Monit. 24 (2018) 567–573, https://doi.org/10.12659/MSM.906708.
[21] H. Ito, M. Maeda, T. Uehara, S. Yamamoto, M. Tamura, T. Takashima, Attenuation values of chronic subdural haematoma and subdural effusion in CT scans, Acta Neurochir. (Wien) 72 (3-4) (1984) 211–217, https://doi.org/10.1007/BF01406871.
[22] J. Stein, K. Huerta, When looking at a non-contrast head CT, what actually appears white in an acute hemorrhagic stroke? Cal. J. Emerg. Med. 3 (4) (2002) 70–71 PMID: 20852704.
[23] G. Boulouis, A. Dumas, R.A. Betensky, H.B. Brouwers, P. Fotiadis, A. Vashkevich, A. Ayres, K. Schwab, J.M. Romero, E.E. Smith, A. Viswanathan, J.N. Goldstein, J. Rosand, M.E. Gurol, S.M. Greenberg, Anatomic pattern of intracerebral hemorrhage expansion: relation to CT angiography spot sign and hematoma center, Stroke 45 (4) (2014) 1154–1156, https://doi.org/10.1161/STROKEAHA.114.004844.
[24] D. Dowlatshahi, J.K. Wasserman, F. Momoli, W. Petrcich, G. Stotts, M. Hogan, M. Sharma, R.I. Aviv, A.M. Demchuk, S. Chakraborty, Evolution of computed tomography angiography spot sign is consistent with a site of active hemorrhage in acute intracerebral hemorrhage, Stroke 45 (2014) 277–280, https://doi.org/10.1161/STROKEAHA.113.003387.
[25] G.N. He, H.Z. Guo, X. Han, E.F. Wang, Y.Q. Zhang, Comparison of CT black hole sign and other CT features in predicting hematoma expansion in patients with ICH, J Neur 265 (8) (2018) 1883–1890, https://doi.org/10.1007/s00415-018-8932-6.
[26] J. Zheng, Xu Z. Yu ZY, M. Li, X.Z. Wang, S. Lin, H. Li, C. You, The accuracy of the spot sign and the blend sign for predicting hematoma expansion in patients with spontaneous intracerebral hemorrhage, Med. Sci. Monit. 23 (2017) 2250–2257, https://doi.org/10.12659/MSM.901583.
[27] P.B. Sporns, M. Schwake, A. Kemmling, J. Minnerup, W. Schwindt, T. Niederatadt, R. Schmidt, U. Hanning, Comparison of Spot Sign, Blend Sign and Black Hole Sign for Outcome Prediction in Patients with Intracerebral Hemorrhage, J. Stroke 19 (3) (2017) 333–339, https://doi.org/10.5853/jos.2016.02061.
[28] R. Wada, R.I. Aviv, A.J. Fox, D.J. Sahlas, D.J. Gladstone, G. Tomlinson, S.P.C.T. Symons, Angiography' 'Spot sign" predicts hematoma expansion in acute intracerebral hemorrhage, Stroke 38 (4) (2007) 1257–1262, https://doi.org/10.1161/01.STR.0000259633.59404.f3.
[29] S.J. Sun, P.Y. Gao, B.B. Sui, X.Y. Hou, Y. Lin, J. Xue, R.Y. Zhai, Dynamic" spot sign" on CT perfusion source images predicts haematoma expansion in acute intracerebral haemorrhage, Eur. Radiol. 23 (7) (2013) 1846–1854, https://doi.org/10.1007/s00330-013-2803-4.
[30] A. Koculym, T.J. Huynh, R. Jakubovic, L. Zhang, R.I. Aviv, CT Perfusion Spot Sign Improves Sensitivity for Prediction of Outcome Compared with CTA and Postcontrast CT, 2013, AJNR Am. J. Neuroradiol. 34 (2013) 965–970, https://doi.org/10.3174/ajnr.a3338.
[31] A.M. Demchuk, D. Dowlatshahi, D. Rodriguez-Luna, C.A. Molina, Y.S. Blas, I. Dzialowski, A. Kobayashi, J.M. Boulanger, C. Lum, G. Gybitz, V. Padma, J. Roy, C.S. Kase, J. Kosior, R. Bhatia, S. Tymchuk, S. Subramaniam, D.J. Gladstone, M.D. Hill, R.I. Aviv, Prediction of haematoma growth and outcome in patients with intracerebral haemorrhage using the CT-angiography spot sign (PREDICT): a prospective observational study, Lancet Neurol. 11 (2012) 307–314, https://doi.org/10.1016/S1474-4422(12)70038-8.
[32] A.D. Giudice, D. D'Amico, J. Sobesky, I. Wellwood, Accuracy of the Spot Sign on Computed Tomography Angiography as a Predictor of Haematoma Enlargement after Acute Spontaneous Intracerebral Haemorrhage: A Systematic Review, Cerebrovasc. Dis. 37 (2014) 268–276, https://doi.org/10.1159/000360754.
[33] X.H. Xu, J.S. Zhang, K. Yang, Q. Wang, B.N. Xu, X.L. Chen, Accuracy of spot sign in predicting hematoma expansion and clinical outcome, Medicine 97 (34) (2018), https://doi.org/10.1097/MD.0000000000011945 (e11945).